

REVIEW PAPER

# Thermography to explore plant–environment interactions

J. Miguel Costa<sup>1,2,\*</sup>, Olga M. Grant<sup>3,4</sup> and M. Manuela Chaves<sup>2</sup>

<sup>1</sup> CBAA, Instituto Superior de Agronomia, Universidade Técnica de Lisboa, Tapada da Ajuda, 1349-017 Lisboa, Portugal

<sup>2</sup> Laboratório de Ecofisiologia Molecular, Instituto de Tecnologia Química e Biológica, Universidade Nova de Lisboa, Av. da República (EAN), 2781-901 Oeiras, Portugal

<sup>3</sup> Department of Biology, National University of Ireland Maynooth, Co. Kildare, Ireland

<sup>4</sup> UCD Forestry, University College Dublin, Dublin 4, Ireland

\* To whom correspondence should be addressed. E-mail: [miguelc@itqb.unl.pt](mailto:miguelc@itqb.unl.pt)

Received 11 October 2012; Revised 9 January 2013; Accepted 15 January 2013

## Abstract

Stomatal regulation is a key determinant of plant photosynthesis and water relations, influencing plant survival, adaptation, and growth. Stomata sense the surrounding environment and respond rapidly to abiotic and biotic stresses. Stomatal conductance to water vapour ( $g_s$ ) and/or transpiration ( $E$ ) are therefore valuable physiological parameters to be monitored in plant and agricultural sciences. However, leaf gas exchange measurements involve contact with leaves and often interfere with leaf functioning. Besides, they are time consuming and are limited by the sampling characteristics (e.g. sample size and/or the high number of samples required). Remote and rapid means to assess  $g_s$  or  $E$  are thus particularly valuable for physiologists, agronomists, and ecologists. Transpiration influences the leaf energy balance and, consequently, leaf temperature ( $T_{\text{leaf}}$ ). As a result, thermal imaging makes it possible to estimate or quantify  $g_s$  and  $E$ . Thermal imaging has been successfully used in a wide range of conditions and with diverse plant species. The technique can be applied at different scales (e.g. from single seedlings/leaves through whole trees or field crops to regions), providing great potential to study plant–environment interactions and specific phenomena such as abnormal stomatal closure, genotypic variation in stress tolerance, and the impact of different management strategies on crop water status. Nevertheless, environmental variability (e.g. in light intensity, temperature, relative humidity, wind speed) affects the accuracy of thermal imaging measurements. This review presents and discusses the advantages of thermal imaging applications to plant science, agriculture, and ecology, as well as its limitations and possible approaches to minimize them, by highlighting examples from previous and ongoing research.

**Key words:** Crop stress, genetic improvement, remote sensing, screening and phenotyping, stomata, thermal infrared.

## Introduction

### *Plant–environment interactions and stomata*

The physical environment is often adverse to plant growth and survival as well as to crop yield and quality. Factors such as insufficient water or nutrients, high or low temperature, salinity, diseases, and insect damage are likely to restrict plant growth at some stage. The predicted global climate change will increase the incidence of extreme climate events (drought spells and heat waves) and related stress, leading to changes in plant biodiversity and reduced crop yields (Fedoroff *et al.*,

2010). Increased sensitivity of crops to pests and diseases and the spread of novel pests and diseases are also likely to occur (Gregory *et al.*, 2009).

Plants interact with the surrounding environment namely through carbon, water- and energy-exchange processes, maintaining an equilibrium that permits them to grow and adapt to variable growing conditions. Stomatal regulation of leaf gas exchange ( $\text{CO}_2$  and  $\text{H}_2\text{O}$  fluxes) in response to the

environment plays a key role in this adaptation, allowing a compromise between photosynthetic gains and water loss as well as allowing regulation of canopy temperature ( $T_{\text{canopy}}$ ) (Jones, 1992; Chaves *et al.*, 2003).

Heat loss by plants occurs mainly via evaporative cooling, resulting from leaf transpiration ( $E$ ) (Jones, 1992). Reduced transpiration under water deficits and high irradiance raises the risk of leaf temperature ( $T_{\text{leaf}}$ ) increasing above the optimum for metabolic activity or above the threshold that leads to irreversible leaf tissue oxidative stress. The control of stomatal aperture results from coordinated alterations of guard cell turgor dependent on ionic fluxes, cytoskeleton changes, membrane transport, and gene expression. This regulation involves the concurrence of different signals in a complex and coordinated network, resulting in a tight and fast modulation of stomatal aperture in response to a fluctuating environment (Hetherington and Woodward, 2003).

If we consider the linear relationship between stomatal conductance to water vapour ( $g_s$ ) and  $E$  under a constant air vapour pressure deficit (VPD), and the non-linear relationship between  $g_s$  and photosynthetic rate, decreased stomatal aperture under the first stages of stress development may improve intrinsic water use efficiency ( $WUE_i$ ) with a positive impact on plant growth and adaptation to the environment. However, when stress becomes severe, a strong decline in carbon assimilation leads to decreased  $WUE_i$ , with photosynthesis being restricted not only by stomatal closure but also by biochemical and photochemical limitations (Chaves *et al.*, 2003).

Regulation of water loss by an efficient control of the opening/closing of stomata also minimizes the risks of xylem embolism by reducing xylem cavitation, and by regulating water fluxes in the plant, indirectly influences water and nutrient uptake. Stomata also influence plant response to biotic stresses. In general, plants respond to surface-inoculated pathogens by reducing stomatal aperture as part of the innate immune response to restrict bacterial invasion (Melotto *et al.*, 2008).

Improved understanding of stomatal regulation of leaf gas exchange is needed to better predict and model key factors influencing crop growth and yield as well as ecosystem sustainability under increasing environmental stress. However, leaf gas exchange measurements involve contact with leaves and often interfere with leaf functioning. Besides, they are time consuming and can be limited by the reduced dimension of the leaf samples and/or the large number of measurements to be done. Therefore, faster, remote and non-invasive high-throughput analysis based on imaging are mandatory.

#### *Remote sensing and functional imaging for plant science*

Remote sensing of vegetation is a non-invasive methodology to monitor physical and physiological characteristics of plants and to evaluate the effects of environmental stresses on plant performance (Jones and Vaughan, 2010). Functional imaging permits observations at different scales (from single leaves/seedlings to entire branches/plants or trees or fields)

and the assessment of dynamic and spatial variability of processes. The basis of nearly all remote sensing is electromagnetic radiation. Remote sensing involves the measurement of the amount of reflected and emitted radiation at different spectral wavelengths (e.g. ultraviolet, visible, infrared (IR), and microwave). It includes several imaging techniques such as visible imaging, near-IR and thermal IR imaging, chlorophyll a fluorescence imaging, and multispectral imaging and luminescence imaging (Chaerle and Van der Straeten, 2001; Baker and Rosenqvist, 2004; Havaux *et al.*, 2006; Lee *et al.*, 2010; Jiménez-Bello *et al.*, 2011; Zarco-Tejada *et al.*, 2012). Among those, thermal imaging (thermography) is one of the most used in agronomic and environmental sciences and also in the agri-food industry (Jones and Vaughan, 2010; Maes and Steppe, 2012).

Remote sensing is the basis of precision agri-horticulture, which aims to use more efficiently the inputs (e.g. water, bio-cides, fertilizers), optimize yield, and minimize environmental impact (Lee *et al.*, 2010). This is in line with the need to increase food production under increasingly unfavourable climate, scarcer natural resources (water, arable land) (Wilkinson and Hartung, 2009; Fedoroff *et al.*, 2010), stricter environmental legislation, and increased consumer demands (Lubin and Esty, 2010).

Remote sensing is also applied in phenomics, an innovative approach towards high-throughput plant phenotyping (Furbank and Tester, 2011), to aid breeding of more productive and stress-resistant cultivars.

### **IR thermal imaging and stomatal conductance**

#### *IR radiation and imaging*

Heat transfer by radiation occurs in the IR region of the electromagnetic spectrum, between 0.75 and 1000  $\mu\text{m}$  (Kaplan, 2007). According to Planck's radiation law, every object at a temperature above absolute zero (0 Kelvin) emits electromagnetic radiation in the IR region of the spectrum. The amount of IR radiation emitted by an object depends on its emissivity ( $\epsilon$ ) and absolute temperature, in accordance with the Stefan–Boltzmann law (Equation 1):

$$W = \epsilon \sigma T_s^4 \quad (1)$$

where  $W$  is spectral radiant excitance (total radiation emitted) ( $\text{W m}^{-2}$ ),  $\epsilon$  is emissivity (dimensionless),  $\sigma$  is the Stefan–Boltzmann constant ( $5.67 \times 10^{-8} \text{ W m}^{-2} \text{ K}^{-4}$ ), and  $T_s$  is the surface temperature (K).

The emissivity, at a particular wavelength, represents the amount of radiation emitted by a theoretical object as a fraction of the radiation emitted by a perfect emitter, named blackbody, with  $\epsilon = 1$ . 'Real-world' objects (grey bodies) absorb a certain fraction of the incident radiation and reflect and transmit the remaining part, resulting in  $\epsilon < 1$ . Plant material has high  $\epsilon$ , varying between 0.91 and 0.97. Soils have slightly lower  $\epsilon$  (0.94–0.95) and sand can have  $\epsilon$  as low as 0.89 (Jones and Vaughan, 2010).

When determining the temperature of an object with thermal imaging, we must consider that the total radiation ( $W$ ) detected by camera's sensor is the sum of three major IR radiation streams: (1) the radiation leaving the object's surface; (2) the radiation emitted by the object's surroundings and further reflected by the object's surface, commonly named background radiation ( $W_{\text{background}}$ ) (both stream 1 and 2 are modified by transmission through the atmosphere); and (3) any radiation emitted by the atmosphere ( $W_{\text{atm}}$ ) (Equation 2). Therefore, the total radiation is given by:

$$W = \tau [\varepsilon \sigma (T_s)^4 + (1 - \varepsilon) W_{\text{background}}] + W_{\text{atm}} \quad (2)$$

where  $\tau$  is atmospheric transmissivity (dimensionless),  $W_{\text{background}}$  is background radiation ( $\text{W m}^{-2}$ ), and  $W_{\text{atm}}$  is the radiance emitted by the atmosphere ( $\text{W m}^{-2}$ ).

The contribution of the atmosphere is relevant for air-borne and satellite measurements (Jones and Vaughan, 2010) but it can be neglected for ground-based measurements and laboratory experiments and when IR radiation is sensed at appropriate wavelengths (e.g. 3–5 and 7–14  $\mu\text{m}$ ), in which the atmospheric transmission for IR radiation is close to a maximum (Kaplan, 2007). In this case the total radiation leaving the surface of the object is calculated as follows:

$$W = \varepsilon \sigma (T_s)^4 + (1 - \varepsilon) W_{\text{background}} \quad (3)$$

To discard the effect of the  $W_{\text{background}}$ , it can be estimated by measuring the temperature of a crumpled sheet of aluminium foil (high reflectivity and  $\varepsilon = 0.03$ ), placed in the same location as the target object and setting the camera with  $\varepsilon = 1$  (Jones *et al.*, 2002). Most thermal cameras will automatically provide  $T_s$ , once the  $\varepsilon$  and  $W_{\text{background}}$  have been input.

#### Relationship between $g_s$ and $T_{\text{leaf}}$

As thoroughly reviewed by Maes and Steppe (2012), leaf and plant temperature depends on the radiation and atmospheric conditions (time of day, clear or cloudy sky, air temperature, wind speed), soil conditions (soil type, soil water content, etc.), and canopy properties (morphology, density, height) that all together influence the size and ratios of the radiant, sensible and latent heat fluxes. The relationship between  $g_s$ , the inverse of stomatal resistance ( $r_s$ , leaf resistance to water vapour loss, assumed to be dominated by the stomatal resistance component), and  $T_{\text{leaf}}$  is summarized by the leaf energy balance equation (Jones, 1992, 1999) given by:

$$T_{\text{leaf}} - T_{\text{air}} = \frac{[r_{\text{HR}} (r_{\text{aw}} + r_s) \gamma R_{\text{ni}} - \rho c_p r_{\text{HR}} \text{VPD}]}{[\rho c_p \{\gamma (r_{\text{aw}} + r_s) + s r_{\text{HR}}\}]} \quad (4)$$

where  $T_{\text{leaf}}$  is leaf temperature (K),  $T_{\text{air}}$  is air temperature (K),  $r_{\text{HR}}$  is parallel resistance to heat and radiative transfer ( $\text{s m}^{-1}$ ),  $r_{\text{aw}}$  is boundary layer resistance to water vapour ( $\text{s m}^{-1}$ ),  $\gamma$  is the psychrometric constant ( $\text{Pa K}^{-1}$ ),  $R_{\text{ni}}$  is net isothermal radiation (the net radiation for a leaf at air temperature) ( $\text{W m}^{-2}$ ),  $\rho$  is density of the air ( $\text{kg m}^{-3}$ ),  $c_p$  is specific heat capacity of air ( $\text{J kg}^{-1} \text{K}^{-1}$ ),  $s$  is the slope of curve relating saturating

water vapour pressure to temperature ( $\text{Pa K}^{-1}$ ), and VPD is air vapour pressure deficit (Pa).

#### Fluctuating environmental conditions and thermal indices

It is clear from Equation 4 that  $T_{\text{leaf}}$  depends not only on  $g_s$ , but also on  $T_{\text{air}}$ ,  $R_{\text{ni}}$ , VPD, and wind speed (Jones, 1999). If comparing, for example, the impact of different management practices on crop physiology while the weather is stable,  $T_{\text{leaf}}$  alone can provide the required information about relative stress in the different treatments. If the aim is to determine the development of stress in a crop over time, on the other hand, it is necessary to normalize  $T_{\text{leaf}}$  in relation to references to account for changing meteorology (Jones *et al.*, 2009). A wide range of different types of stress index have been used to address this issue. Here an overview is provided to allow the reader to determine what technique might suit a particular experiment. For more detailed assessment of the pros and cons of each, including analysis of the impact of such factors as leaf size and albedo,  $T_{\text{air}}$  and VPD, and  $R_{\text{ni}}$ , see Maes and Steppe (2012).

That  $T_{\text{leaf}}$  increases as a result of stress was first exploited by Jackson *et al.* (1977), who developed the stress degree day to detect stress by using thermometers in field conditions. The stress degree day is the accumulated difference in temperature between the leaf (or crop canopy) and the air along a certain period. According to this index, if  $T_{\text{canopy}}$  is lower than  $T_{\text{air}}$ , then plants are assumed to be well watered. If  $T_{\text{canopy}}$  is greater than the  $T_{\text{air}}$ , then plants are assumed to be drought stressed. While this index represents an improvement over the use of  $T_{\text{canopy}}$  alone, since it allows for fluctuating  $T_{\text{air}}$ , it does not take into account changes in VPD, solar radiation, or wind speed.

Based on energy balance considerations, Jackson *et al.* (1981) appreciated that the canopy to air temperature difference ( $T_{\text{canopy}} - T_{\text{air}}$ ) depends on VPD: under non-limiting soil water conditions, a crop transpires at the potential rate (i.e. evapotranspiration is the maximum it can be, but maximum evapotranspiration increases with increasing VPD). Thus for several crops, when water availability is not limiting and when measured under clear sky conditions, there is a linear relationship between  $T_{\text{canopy}} - T_{\text{air}}$  and VPD. Jackson *et al.* (1981) called this linear relationship the theoretical non-water-stressed baseline. For a given crop, at a given VPD, this theoretical baseline provides the minimum possible value of  $T_{\text{canopy}} - T_{\text{air}}$ . The  $T_{\text{canopy}} - T_{\text{air}}$  for a non-transpiring crop is insensitive to VPD, and can be estimated if wind speed and net solar radiation are known. This sets the 'upper limit' to  $T_{\text{canopy}} - T_{\text{air}}$ . Jackson *et al.* (1981) used the idea of 'upper and lower' baselines, to create a crop water stress index (CWSI):

$$CWSI = \frac{(T_{\text{canopy}} - T_{\text{air}}) - (T_{\text{canopy}} - T_{\text{air}})_{\text{nwsb}}}{(T_{\text{canopy}} - T_{\text{air}})_{\text{ul}} - (T_{\text{canopy}} - T_{\text{air}})_{\text{nwsb}}} \quad (5)$$

where  $T_{\text{canopy}} - T_{\text{air}}$  is the measured difference in temperature,  $(T_{\text{canopy}} - T_{\text{air}})_{\text{nwsb}}$  is the estimated difference at the same



VPD under non-limiting soil water conditions (non-water-stressed baseline), and  $(T_{\text{canopy}} - T_{\text{air}})_{\text{ul}}$  is the non-transpiring upper limit. This CWSI allows to relate crop's temperature to the maximum and minimum values possible under similar environmental conditions. The higher the CWSI, the greater the crop stress is assumed to be. Yuan et al. (2004) and Testi et al. (2008) for example, found CWSI to be inversely correlated with leaf water potential.

A disadvantage of the above form of CWSI is the need to determine the non-water-stressed baseline by plotting  $T_{\text{canopy}} - T_{\text{air}}$  against VPD. This requires substantial time to be spent determining the baseline for a well-watered crop, and the VPD needs to be known when measuring  $T_{\text{canopy}}$  of the crop of interest. Also, this index does not account for changes in  $T_{\text{canopy}}$  due to irradiance and wind speed, and the non-water-stressed baseline is not necessarily the same under different radiation conditions. Finally, the non-transpiring upper limit also varies, with a wide range of values being reported (Ben-Gal et al., 2009).

#### Use of artificial references

An alternative approach is to replace the non-water-stressed baseline and the non-transpiring upper limit, respectively, with the  $T_{\text{leaf}}$  or  $T_{\text{canopy}}$  from which there is maximum transpiration and the  $T_{\text{leaf}}$  and  $T_{\text{canopy}}$  from which there is no transpiration, measured in the same environment and at the same time as the crop of interest. The fact that these 'references' are in the same environment as  $T_{\text{canopy}}$  means that there is no need for theoretical estimations of baselines, as they will be exposed to the same VPD,  $R_{\text{ni}}$ , and wind speed as the canopy of interest. The temperatures of the references are referred to as  $T_{\text{wet}}$  and  $T_{\text{dry}}$ , respectively. Jones (1999) adapted the crop water stress index to include these reference temperatures, giving the following form:

$$\text{CWSI} = \frac{(T_{\text{canopy}} - T_{\text{wet}})}{(T_{\text{dry}} - T_{\text{wet}})} \quad (6)$$

This version of CWSI (referred to as  $\text{CWSI}_d$  in the review by Maes and Steppe, 2012) has been shown to inversely correlate with leaf water potential (e.g. Cohen et al., 2005; Grant et al., 2007). To ensure that there are suitable references in each thermal image, leaves can be sprayed with water ( $T_{\text{wet}}$ ) and covered in Vaseline to artificially close stomata ( $T_{\text{dry}}$ ) (Fig. 1A–C). Other approaches include the use of wet and dry filter paper (Jones et al., 2002; Loveys et al., 2008), wet and dry cotton (Fig. 1D, E), and wet and dry tensiometers (Fig. 1F, G). Metal artificial leaves can be used as well (Fig. 1H, I). To prevent the wet reference from drying out, sometimes a reservoir of water is provided, with material acting as a wick (Alchanatis et al., 2010).

An alternative index, based on a rearrangement of the energy balance equation, is thermal index of relative stomatal conductance ( $I_G$ ) (Jones, 1999):

$$I_G = \frac{(T_{\text{dry}} - T_{\text{canopy}})}{(T_{\text{canopy}} - T_{\text{wet}})} \quad (7)$$

For most values of  $g_s$ ,  $I_G$  is linearly proportional to  $g_s$ , as has now been demonstrated under a wide range of conditions (as reviewed by Maes and Steppe, 2012). This index uses the same references as the second form of CWSI (Equation 6), but gives low values in stressed crops and higher values with increasing  $g_s$ .

As the inclusion of wet and dry reference surfaces in every image can sometimes be logistically difficult, an alternative to the above indices is to use an actual non-water-stressed plant/crop and a stressed plant/crop as extremes and relate the temperature of the crop of interest to these (Grant et al., 2007). This is appropriate for example where the crop of interest is deficit irrigated and hence expected to have a  $T_{\text{canopy}}$  intermediate between those extremes. Since the reference crops, however, cannot usually be included in every image, there is the problem that meteorological conditions can change between imaging the reference crop and the crop of interest. Grant et al. (2007) therefore interpolated the temperatures of the reference crops between a series of images to estimate their temperature at the precise time at which the crops of interest were imaged.

#### Separating canopy from soil temperature

The above indices are appropriate where only leaves are being analysed (i.e. either the crop completely covers the soil, or only leaves are selected to acquire  $T_{\text{canopy}}$ ). An alternative index called the water deficit index (WDI) was developed for applications where soil and crop temperatures could not be separated (Moran, 1994). This index uses the difference between the temperature of the surface (which includes vegetation and bare soil) and the temperature of the air –  $(T_s - T_{\text{air}})$  – along with an index of vegetation cover. At 100% vegetation cover, the values of WDI will fall within the same limits of the CWSI. For more details on the estimation and the pros and cons of the WDI, see Maes and Steppe (2012).

#### Alternatives to the stress indices

An alternative to the use of stress indices is to estimate  $g_s$  (Leinonen et al., 2006; Guillioni et al., 2008) from  $T_{\text{leaf}}$ . This requires that  $T_{\text{air}}$  and VPD, net radiation, and wind speed are measured at the same time as  $T_{\text{leaf}}$ . Berni et al. (2009) used this approach to estimate canopy conductance of olive trees under different irrigation regimes, with  $T_{\text{leaf}}$  being derived from an image obtained from an unmanned aerial vehicle (UAV). They also estimated CWSI using meteorological data rather than references to obtain  $T_{\text{wet}}$  and  $T_{\text{dry}}$ , and found that the estimated CWSI was strongly inversely correlated with leaf water potential. Ben-Gal et al. (2009) compared estimation of CWSI using meteorological data with estimation using  $T_{\text{dry}} = T_{\text{air}} + 5^\circ\text{C}$  (which is rather arbitrary) and  $T_{\text{wet}}$  being the temperature of a wet cloth. The two methods gave similar results, and the authors suggest using meteorological data is preferable, to avoid the need of a wet reference in every image. This approach, however, does mean that the reference temperatures are not obtained at the same environmental conditions as  $T_{\text{leaf}}$ , since a full set of meteorological data cannot be collected at each plant of interest.

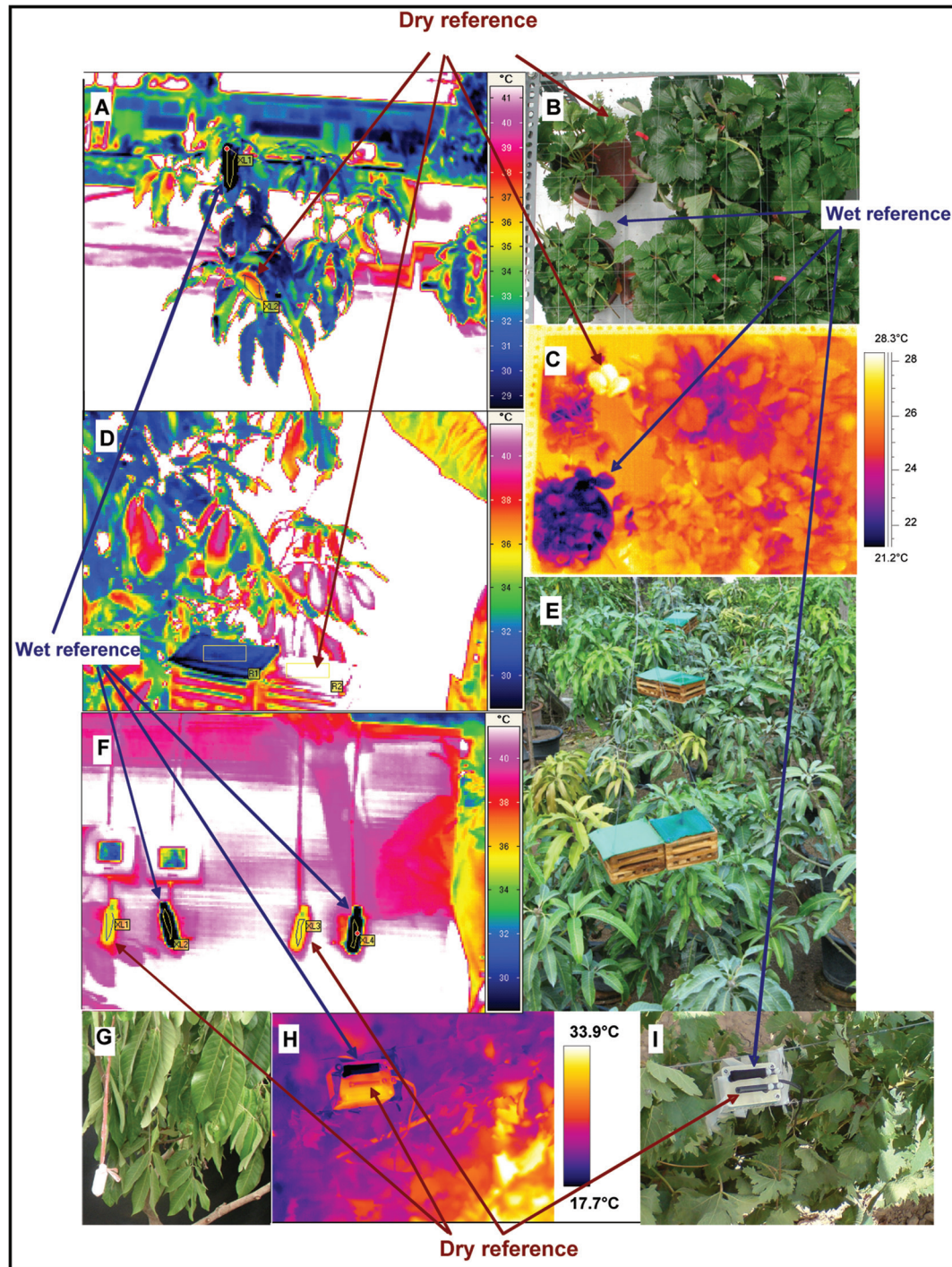


**Fig. 1.** Different approaches to providing wet and dry reference surfaces to estimate  $T_{\text{wet}}$  and  $T_{\text{dry}}$ . (A–C) Wet and dry leaves on the plant of interest. (D, E) Wet and dry cotton material covering pairs of reservoirs (D), with the reservoir filled with water in the case of the wet reference and left empty in the case of the dry reference – such a system can be hung from trees (E). (F, G) Wet and dry tensiometers (F), which can also be hung from trees (G). (H, I) Wet and dry artificial leaves of a sensor designed to monitor wet leaf depression (Evaposensor, Skye Instruments, Powys, UK): the artificial leaves are metal, but the wet artificial leaf is kept wet by means of a wick in a reservoir of water. Images A, D, F, and H were taken with IR cameras; all others are RGB digital images; images relate to various projects, with participation of U Srikasetsarakul, W Spreer, S Zia (A, D–G), and H Ochagavía (H, I), and funding from sources including Deutsche Forschungsgemeinschaft (A, D–G) and the UK Department of the Environment, Food and Rural Affairs (B, C).

A compromise is to use one reference: if  $T_{\text{dry}}$  is measured, then the need to measure net radiation is removed – an approach that gave consistent results in both field (Leinonen

*et al.*, 2006) and greenhouse (Grant *et al.*, 2012) conditions. If  $T_{\text{wet}}$  is also measured,  $T_{\text{air}}$  and the boundary layer resistance are the only additional information required to estimate  $g_s$ .



Some authors have empirically determined the relationship between CWSI and leaf water potential, or between  $T_{\text{canopy}}$  and stem water potential or  $g_s$ , and then used this relationship to map variation in water potential or  $g_s$  (Cohen *et al.*, 2005; Alchanatis *et al.*, 2010; Baluja *et al.*, 2012). The step of determining the empirical relationship for a subsample is not necessary because  $g_s$  can be mapped from  $T_{\text{leaf}}$  based simply on Equation 4.

A different approach is to focus on variability of temperature, rather than absolute temperature. Given the large influence of  $g_s$  on the energy budget of a canopy, a greater range of temperatures will be found in a canopy as stomata close, due to the relatively greater influence of variation in leaf exposure as compared to a non-stressed, fully transpiring canopy (Fuchs, 1990). This, however, will not apply to canopies with a non-random distribution of leaf exposure (Grant *et al.*, 2007). There has been little experimental assessment of this approach with canopies that do show a random distribution of leaf angle and orientation, with the exception of a study by Bryant and Moran (1999), which showed that crop temperatures deviate from a normal distribution as plant water stress increases.

González-Dugo *et al.* (2006) considered that variation in temperature in a crop will increase with stress not because of increased variation in leaf exposure when transpiration is low, but because variability in rooting depth or soil structure, for example, will increase as soil dries. They therefore compared the standard deviation of  $T_{\text{canopy}}$  to that of CWSI and found that the standard deviation of  $T_{\text{canopy}}$  correlates with CWSI for moderate but not for severe water stress.

## Thermal imaging: applications in plant and agricultural sciences

### *Forward genetics screens and characterization of mutants and transgenics*

Forward genetics and selection of stomatal mutants has been providing new biological tools to study and better understand the genetic, physical, and physiological basis of stomatal responses to environment (Papdi *et al.*, 2009; Dodd, 2013). Forward genetics involves induction of artificial genetic variation by chemical, physical, or biological mutagenesis and the screening of mutants for a certain phenotype of interest (Papdi *et al.*, 2009). Mutants identified in novel screens are useful to identify signalling pathway components and potential genes that can be used to improve plant performance under stress (e.g. drought) (Plessis *et al.*, 2011). The use of thermal imaging in forward genetics and related large-scale screens and mutant characterization is rather recent (Merlot *et al.*, 2002) and accompanied rapid developments in plant molecular physiology and functional genomics. In the context of studies on stomatal regulation, the aim of forward genetics is to dissect different signalling pathways (e.g. abscisic acid) at the genetic level involved in regulation of guard cell response to internal and environmental signals.

With thermal imaging it is possible to screen several thousands of young seedlings and isolate those presenting a

temperature difference relative to the respective wild type, as a result of different stomatal regulation (example in Fig. 2A). The model species *Arabidopsis thaliana* has been used to identify and characterize molecular regulators of transpiration using forward genetics (Nilsson and Assmann, 2007). Mutants with abnormal stomatal response to drought (Merlot *et al.*, 2002; Plessis *et al.*, 2011), light (Merlot *et al.*, 2007), air CO<sub>2</sub> concentration (Hashimoto *et al.*, 2006), air VPD (Xie *et al.*, 2006) and ozone (Saji *et al.*, 2008) have been isolated to date. Genetic characterization of these mutants led to the identification of new genes encoding proteins such as an abscisic acid-activated protein kinase (Merlot *et al.*, 2002) and a plasma membrane H<sup>+</sup>-ATPase (Merlot *et al.*, 2007), as well as other key mediators involved in signalling networks regulating stomatal aperture/closure in response to the environment (Papdi *et al.*, 2009; Sirichandra *et al.*, 2009). For example, Merlot *et al.* (2002) isolated mutations at two novel loci designated as *OST1* (OPEN STOMATA 1, At4g33950) and *OST2*. *ost1* and *ost2* were the first mutations altering abscisic acid responsiveness in stomata and not in seeds (Merlot *et al.*, 2002). More recently, Negi *et al.* (2008) isolated another *Arabidopsis* gene, *SLAC1* (SLOW ANION CHANNEL-ASSOCIATED 1, At1g12480), encoding the S-type anion channel, which was shown to mediate sensitivity of stomata to CO<sub>2</sub>. *SLAC1* was found essential for stomatal closure in response to CO<sub>2</sub>, and *SLAC1*-deficient mutants showed constitutively higher  $g_s$  as result of larger stomatal aperture.

In rice, thermography helped to isolate and characterize *SLAC1*-deficient mutants with a constitutive low  $T_{\text{leaf}}$  phenotype and consequently higher  $g_s$  (Kusumi *et al.*, 2012). These mutants had higher photosynthetic rates than the wild type, which could improve growth and yield. Transgenic lines of rice overexpressing a transcription factor (bHLH family) were characterized for their response to drought stress. The overexpressing line showed lower  $T_{\text{leaf}}$  (and consequently higher  $g_s$ ) than the silencing line (Chander *et al.*, unpublished) (Fig. 2B).

Thermal imaging is also useful to support preliminary physiological characterization of novel mutants with abnormal leaf growth (small and curled leaves), which limit leaf gas exchange measurements. Characterization of *ESK1*, which results in reduced growth and deficient vascular water transport, was based on measurements of  $T_{\text{leaf}}$  in detached leaves (Lefebvre *et al.*, 2011).

### *Stress detection and management*

#### *Water stress monitoring and irrigation management*

Given the relationship between  $T_{\text{leaf}}$  and crop stress, the potential of thermal imaging to monitor crop water status is clear. In fact, thermal imaging can show differences between irrigated and non-irrigated plants and between different intensities of irrigation (Cohen *et al.*, 2005; Grant *et al.*, 2007; Möller *et al.*, 2007; Berni *et al.*, 2009; Padhi *et al.*, 2012; Zarco-Tejada *et al.*, 2012). In some cases, a single thermal image is sufficient to reveal spatial variation in plant water status. On a larger scale, aerial thermal imaging is used to detect variation in crop water status at a single point in time. In this case, resolution is critical: Berni *et al.* (2009) were able to determine the temperature

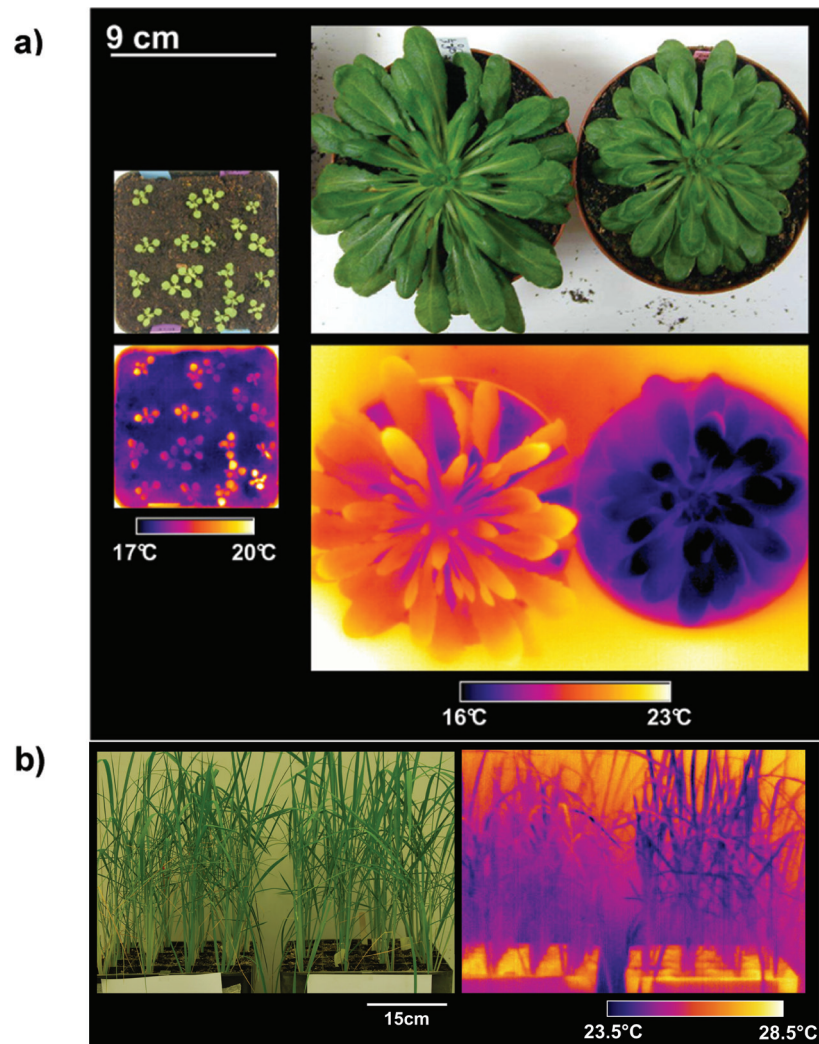


**Fig. 2.** Examples of thermal imaging in forward genetics and plant phenotyping. A: Visible (upper) and false-coloured thermal (lower) images at two growth stages (young seedlings and mature stage), for wild type (WT, ecotype Columbia) (left) and mutant *ost2* (Merlot *et al.*, 2007) (right) *Arabidopsis thaliana* after plants were dark adapted. The WT close their stomata in the dark whereas the *ost2* plants do not. Therefore, the WT show higher leaf temperatures than mutants. (B) Visible and false coloured IR images of 4-week-old rice plants subjected to drought and overexpressing (right) and silencing (left) a bHLH transcription factor (Chander S, Almeida D, Serra T, Barros P, Costa JM, Santos T, Oliveira MM, Saibo N, unpublished, with permission).

of individual trees from a thermal image taken from an UAV, providing a resolution of 40 cm; this was not possible when thermal images were taken from a higher-flying aeroplane that provided a resolution of only 2 m.

The greatest temperature differences between stressed and non-stressed canopies are found in hot, dry environments. There are limitations concerning measurements in more humid areas with low leaf-to-air vapour pressure differences (Thomson *et al.*, 2012). Nevertheless, detectable differences were measured under relatively humid, cool, and low radiation conditions, as noted by Maes and Steppe (2012).

The capacity of thermal imaging to detect variation in crop water status depends on the plant's stomatal response. In species with more marked anisohydric behaviour (e.g. sunflower, wheat, soybean, almond tree), leaf water potential falls with increasing evaporative demand (Tardieu and Simonneau, 1998), due to poor stomatal control over tissue water loss.

For this reason, in these species leaf water potential is a better indicator of soil moisture than  $g_s$ . Isohydric species (e.g. maize, lupin, pea, poplar), on the other hand, close their stomata in response to a decrease in soil water and/or an increase in VPD, controlling plant water potential. Under such conditions,  $g_s$  is a better indicator of soil moisture than water potential. Therefore, drought detection using thermal imaging is more suited to species or varieties exhibiting isohydric behaviour (Jones *et al.*, 2009).

A logical step forward for the use of this methodology is to use thermal imaging to decide where, when, and how much to irrigate. This, however, requires that a threshold for crop temperature, a stress index, or a value of  $g_s$  is established beforehand. Irrigation would be applied when this threshold is reached. Threshold values may vary according to the environment and species or variety/cultivar (Cohen *et al.*, 2005; Möller *et al.*, 2007; Costa *et al.*, 2012; Fuentes *et al.*, 2012).



Further progress is still required before thermal imaging is routinely used for irrigation scheduling. There is the need for monitoring crops over the whole season and ultimately compare thermography with other scheduling methods. Where the costs involved in frequent thermal imaging are prohibitive, infrequent thermal imaging (e.g. aerial or satellite) that will provide information on spatial variation may be combined with frequent (or continuous) alternative means of monitoring water stress. The latter would provide poor spatial resolution, but high temporal resolution. For example, a single aerial or satellite image may be sufficient to pinpoint areas of a crop with different water demands, and representative plants within each zone could then be continuously monitored (e.g. by measuring stem diameter fluctuations or sap flow) in order to schedule irrigation over a season. [García-Tejero \*et al.\* \(2011\)](#) suggested that the combined monitoring of maximum daily trunk shrinkage (to obtain information regarding individual plants) and  $T_{\text{canopy}} - T_{\text{air}}$  (to obtain information regarding plots) would help to determine irrigation requirements in orchards with spatial variation in plant water status. Aerial and ground thermal imaging can also support detection of malfunctioning (e.g. leaks) of irrigation canals and delivery systems, which result in large water losses ([Thomson \*et al.\*, 2012](#)).

#### Crop protection

Pests and diseases limit the genetic potential of crops regarding their growth and yield. Pests and diseases can change the amount and direction of radiation reflected and emitted by plants ([Jackson, 1986](#)) or can modify plant temperature due to stomatal deregulation and/or changes in plant water relations ([Nilsson, 1995](#); [Allègre \*et al.\*, 2007](#)). Thermal imaging can thus be used to monitor infection patterns of diseases or infestation by pests, which assume typical patchy distributions ([Mahlein \*et al.\*, 2012](#)), or even to detect the stress before symptoms are visible ([Jackson, 1986](#); [Nilsson, 1995](#); [Oerke \*et al.\*, 2006](#); [Stoll \*et al.\*, 2008](#); [Chaerle \*et al.\*, 2009](#)).

Increase in plant temperature can co-occur with senescence due to biotic stress, resulting from modified plant–water relationships due to the interruption of normal function of the root system or/and blockage of water and nutrient transport in the stem or leaves ([Nilsson, 1995](#)). Foliar pathogens can disrupt cuticular and/or stomatal regulation of transpiration and influence plant water relations and  $WUE_i$  ([Grimmer \*et al.\*, 2012](#)). Thermal imaging also supports studies of the action of herbivorous insects: for example, transpirational water loss in soybean (*Glycine max*) leaflets occurred mostly from injuries on cuticle and cut edges of the attacked leaves ([Aldea \*et al.\*, 2005](#)).

Combined thermal imaging and gas exchange studies under laboratory conditions showed that the accumulation of salicylic acid (a hormone produced in plant defence against infections) in response to tobacco mosaic virus infection in tobacco leaves was paralleled by stomatal closure:  $T_{\text{leaf}}$  increased after virus inoculation prior to cell death ([Chaerle \*et al.\*, 1999](#)). However, if the infection has only a minor effect on transpiration, detection using thermography may not be possible, particularly in field conditions.

Moreover, combination of stresses can also pose limitations when monitoring infection with thermal imaging. For example, in grapevine, the maximum temperature difference between infected and non-infected areas reached 0.9 °C in irrigated plots, but only 0.3 °C for non-irrigated plots ([Stoll \*et al.\*, 2008](#)). Although there are limitations in the identification of the causal agent of biotic stress (disease, pest) ([Jackson, 1986](#)), thermal imaging can be used in field conditions to localize spots where the crop is more affected and demanding more urgent intervention ([Sankaran \*et al.\*, 2010](#)).

#### Other stresses

[Shimshi \(1967\)](#) observed that, under conditions favouring stomatal opening (non-limiting soil moisture content) nitrogen and iron deficiency would induce stomatal closure in different crop species (e.g. beans, wheat, sugar beets, maize, groundnuts). Under controlled conditions, [Chaerle \*et al.\* \(2007\)](#) using thermal imaging showed that bean plants growing on magnesium deficient solution had a higher temperature (by about 0.5 °C) compared to control plants. Preliminary thermal imaging of spring barley also indicated higher canopy temperature in crops that did not receive any nitrogen fertilizer compared to those that were well fertilized (165 kg N ha<sup>-1</sup>; [Fig. 3](#)). This suggests stomatal closure in the nutrient-starved crops. On the contrary, wheat plants growing under higher nitrogen conditions for two consecutive years exhibited lower  $T_{\text{canopy}}$  ([Tilling \*et al.\* 2007](#)). In field measurements, combining thermal and spectral properties of canopies may help to identify more precisely nutrient deficiency and distinguish between water and nutrient stress ([Christensen \*et al.\*, 2005](#)).

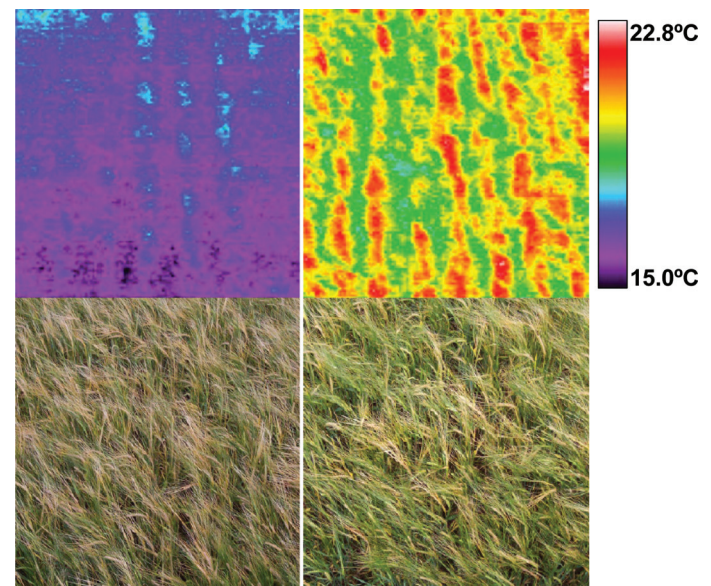


**Fig. 3.** Spring barley crops subjected to a high nitrogen fertilizer input (165 kg N ha<sup>-1</sup>; left) and no nitrogen fertilizer (right), and imaged with an IR Snapshot 525 (Infrared Solutions, Minneapolis, USA) 120 × 120 pixel line scan imager, 8–12 μm (top) and a digital camera (bottom) from a ladder, showing higher crop temperature in the nitrogen-deprived crop.



In *Trifolium subterraneum*, ozone exposure resulted in higher  $T_{\text{leaf}}$  in long-day plants as compared to short-day plants, suggesting that ozone reduces  $E$  in long-day plants (Vollnes *et al.*, 2009). Energy released during freezing results in an increase of temperature, which can be recorded by thermal imaging (Wisniewski *et al.*, 2008), with the advantage over contact thermometry of detecting the actual site of ice initiation and the number of ice nucleation events. The technique has been applied to study frost resistance in woody plants (Pramsohler *et al.*, 2012).

### Crop phenotyping and breeding

The ultimate goal of phenotyping in plant breeding is to quantify and rank the success of a range of genotypes in certain environments (Walter *et al.*, 2012). It involves comparison of large numbers of genotypes, which requires fast and robust measurement procedures, with a high degree of automation (Roy *et al.*, 2011; Walter *et al.*, 2012).

Novel crop genotypes are often characterized on the basis of leaf gas exchange traits (e.g. photosynthetic assimilation,  $g_s$ ,  $\text{WUE}_i$ ). Thermal imaging emerged as a faster method to carry out high-throughput field phenotyping compared to point measurements of  $T_{\text{leaf}}$ , porometry, or leaf gas exchange (Furbank and Tester, 2011; Walter *et al.*, 2012). Besides, it allows phenotyping of different sized plants (small seedlings to entire plants/canopies) in controlled or field conditions (Jones *et al.*, 2009; Walter *et al.*, 2012). Genotypes of different crops have been characterized in their response to different environmental stresses using thermal imaging (Munns *et al.*, 2010; Walter *et al.*, 2012).

High-yielding rice cultivars have been selected on the basis of their lower  $T_{\text{leaf}}$  and higher canopy diffusive conductance to water vapour (Jones *et al.*, 2009; Berger *et al.*, 2010), and several quantitative trait loci for  $T_{\text{leaf}}$  differences have been mapped in relation to stomatal behaviour traits (Pelleschi *et al.*, 2006). In maize, lower  $T_{\text{leaf}}$  was positively correlated with biomass accumulation under water stress, supporting the use of thermal imaging in breeding and selection of drought tolerant maize genotypes (Liu *et al.*, 2011). The low  $T_{\text{canopy}}$  of resistant lines observed under drought stress is an indicator of plant water status and of drought-avoidance mechanisms and may be related to deep root growth that allow plants to continue water uptake and transpiration that cools the leaves (Jones *et al.*, 2009; Henry *et al.*, 2011).

In strawberry, thermal imaging indicated that some cultivars display low  $g_s$  whereas others show high  $g_s$  under similar well-watered conditions (Grant *et al.*, 2012). In grapevine, thermal imaging can also be used in breeding programmes for  $\text{WUE}_i$  since both  $g_s$  and photosynthetic assimilation are genetically dependent traits in this species (Flexas *et al.*, 2010). Recently, Costa *et al.* (2012) observed different  $T_{\text{leaf}}$  and  $g_s$  phenotypes between grapevine varieties with similar water status, suggesting different types of stomatal regulation.

High-resolution thermal imaging can also help to characterize morphology and plant architecture traits that are important for selecting superior varieties for different environmental conditions (Chéné *et al.*, 2012).

### Ecological studies and environmental monitoring

Remote sensing has been used by ecologists and conservation biologists in larger scale studies to better understand environmental changes and their consequences in plant ecosystems (Jones and Vaughan, 2010). Thermal remote sensing allows monitoring of physiological activity of vegetation (Jacob *et al.*, 2008), and satellite thermal sensing has been used to support modelling of regional fluxes of water and mapping of evapotranspiration and moisture availability (Anderson *et al.*, 2008; Chávez *et al.*, 2008; Sobrino *et al.*, 2009), as well as in monitoring drought and water use, administering irrigation projects, predicting local and regional water demand, and supporting hydrological and weather forecast models (Anderson and Kustas, 2008).

Scherrer and Körner (2010) have used thermal imaging to monitor alpine landscapes over time with very high spatial resolution. They quantified variation between microhabitats by the deviation of vegetation surface temperature from  $T_{\text{air}}$ . This is an advance compared to previous approaches based on conventional climate station data that only enabled monitoring of individual plants or soil plots. More recently, Scherrer and Körner (2011) used high-resolution IR thermal imaging to assess the spatial and temporal variation of plant surface and ground temperatures for hundreds of plots distributed across three alpine slopes of contrasting exposure. The results emphasize the need to take microhabitat temperature variation into account when predicting climate change impacts on vegetation: meter-scale thermal contrasts were far greater than the average increase in temperature predicted for the next 100 years.

Scherrer *et al.* (2011) established a drought-sensitivity ranking of deciduous tree species based on thermal imaging and found that in drier sites and at higher temperatures some species could be less competitive than others. Pronounced drought might change the competitive abilities of tree species in favour of those that are able to maintain transpirational fluxes and cooler canopies, such as *Fraxinus excelsior* and *Quercus petraea*. Complementary ground thermal imaging at key locations could enhance the usefulness of satellite sensing (Qiu and Zhao, 2010), namely in ecology (Kerr and Ostrovsky, 2003), by providing the fine local resolution that satellite imaging cannot.

### Other applications in agro-food industries

Thermal imaging can be used to monitor quality of horticultural products, namely seed viability (Kranter *et al.*, 2010), health of transplants (Kim and Lee, 2004), and graft union quality (Torii *et al.*, 1992). In orchards and groves, thermal imaging can help to assess fruit number (Bulanon *et al.*, 2008). Additionally, thermal imaging of fruits under field conditions could assist in understanding the impact of extreme temperatures on fruit quality, namely on the incidence/resistance to sunscald (yellowing/browning of a fruit's skin and softened flesh from exposure to high temperatures) (Prohens *et al.*, 2004).

Thermal imaging can also support optimized climate control in greenhouse horticulture. Greenhouse climate control could be based on continuous measurements of  $T_{\text{leaf}}$  instead

of  $T_{\text{air}}$  because  $T_{\text{leaf}}$  is more closely linked to plant performance (Ehret *et al.*, 2001).

## Future prospects

As advances in detector technology and progress in image processing increase the diagnostic power of thermal imaging, the main challenge may shift from such technical aspects to the optimization of data collection. Physiologically, there is still a need to establish leaf/canopy thresholds (thresholds of relevant thermal indexes) for different biotic or abiotic stress effects and for different species and varieties. Studies that deal with a longer time scale are required as well, rather than mere correlations between temperature variables and standard indicators of stress based on measurements on single dates.

Technologically, future developments will include the combination of thermal imaging with imaging in other spectral wavelengths (visible and red/infrared reflectance, chlorophyll fluorescence) (Bulanon *et al.*, 2008; Jiménez-Bello *et al.*, 2011). The use of UAVs for civil applications opened up a new era of remote sensing, aiding assessment of plant–environment interactions at a larger scale (e.g. crop fields and forest plots) (Berni *et al.*, 2009), although there exists legal restrictions in its use in many countries. Coupling of ground and airborne measurements must be improved, in order to increase the accuracy of retrieved data. Thermal imaging in parallel with wireless sensor networks and geographical information systems will allow a more precise mapping and monitoring of, for example, irrigation and fertilizer requirements (Lee *et al.*, 2010).

Coupling of thermal imaging with modelling approaches is expected (Maes and Steppe, 2012), which should be supported by improved software tools to optimize automation and speed up robust image analysis (Fuentes *et al.*, 2012).

With respect to routine application in the land-based industry sector, as opposed to scientific research, enhanced benefits will arise from reduction in costs of thermal imaging devices that will permit extending the use of the technique in agronomy to a wider range of crops and situations than only the most advanced and intensive agricultural/horticultural systems.

## Acknowledgements

JMC was supported by a post-doctoral fellowship granted by Fundação para a Ciência e Tecnologia (ref. no. SFRH/BPD/34429/2006) and OMG received an EU Marie Curie Intra-European Fellowship (grant no. 252196). The authors thank Bernard Genty for providing the thermal image of the *ost2.2* mutant and acknowledge funding from the EU-STRESSIMAGING project, the EU project SWUPMED (KBBE-2008-212337), and the FCT projects PTDC/AGR-ALI/100636/2008 and PEst-OE/EQB/LA0004/2011.

## References

Alchanatis V, Cohen Y, Cohen S, Moller M, Sprinstin M, Meron M, Tsipris J, Saranga Y, Sela E. 2010. Evaluation of different

approaches for estimating and mapping crop water status in cotton with thermal imaging. *Precision Agriculture* **11**, 27–41.

Aldea M, Hamilton JG, Resti JP, Zangerl AR, Berenbaum MR, DeLucia EH. 2005. Indirect effects of insect herbivory on leaf gas exchange in soybean. *Plant, Cell and Environment* **28**, 402–411.

Allègre M, Daire X, Héloir MC, Trouvelot S, Mercier L, Adrian M, Pugin A. 2007. Stomatal deregulation in *Plasmopara viticola*-infected grapevine leaves. *New Phytologist* **173**, 832–840.

Anderson MC, Kustas WP. 2008. Thermal remote sensing of drought and evapotranspiration. *EOS Transactions American Geophysical Union* **89**, 233–240.

Anderson MC, Norman JM, Kustas WP, Houborg R, Starks PJ, Agam N. 2008. A thermal-based remote sensing technique for routine mapping of land-surface carbon, water and energy fluxes from field to regional scales. *Remote Sensing of Environment* **112**, 4227–4241.

Baker N, Rosenqvist E. 2004. Applications of chlorophyll fluorescence can improve crop production strategies: an examination of future possibilities. *Journal of Experimental Botany* **55**, 1607–1621.

Baluja J, Diago MP, Zorer R, Meggio F, Tardaguila J. 2012. Assessment of vineyard water status variability by thermal and multispectral imagery using an unmanned aerial vehicle (UAV). *Irrigation Science* **30**, 511–522.

Ben-Gal A, Agam N, Alchanatis V, Cohen Y, Yermiyahu U, Zipori I, Presnov E, Sprinstin M, Dag A. 2009. Evaluating water stress in irrigated olives: correlation of soil water status, tree water status, and thermal imagery. *Irrigation Science* **27**, 367–376.

Berger B, Parent B, Tester MA. 2010. High-throughput shoot imaging to study drought responses. *Journal of Experimental Botany* **61**, 3519–3528.

Berni JAJ, Zarco-Tejada PJ, Suárez L, Fereres E. 2009. Thermal and narrowband multispectral remote sensing for vegetation monitoring from an unmanned aerial vehicle. *Transactions on Geoscience and Remote Sensing* **47**, 722–738.

Bryant RB, Moran MS. 1999. *Determining crop water stress from crop temperature variability*. Ottawa: International Airborne Remote Sensing Conference, Canadian Remote Sensing Society.

Bulanon DM, Burks TF, Alchanatis V. 2008. Study on temporal variation in citrus canopy using thermal imaging for citrus fruit detection. *Biosystems Engineering* **101**, 161–171.

Chaerle L, Hagenbeek D, Vanrobaeys X, Van Der Straeten D. 2007. Early detection of nutrient and biotic stress in *Phaseolus vulgaris*. *International Journal of Remote Sensing* **28**, 3479–3492.

Chaerle L, Lenk S, Leinonen I, Jones HG, Van Der Straeten D, Buschmann C. 2009. Multi-sensor plant imaging: towards the development of a stress-catalogue. *Biotechnology Journal* **4**, 1152–1167.

Chaerle L, Van Caeneghem W, Messens E, Lambers H, Van Montagu M, Van Der Straeten D. 1999. Presymptomatic visualization of plant–virus interactions by thermography. *Nature Biotechnology* **17**, 813–816.

Chaerle L, Van Der Straeten D. 2001. Seeing is believing: imaging techniques to monitor plant health. *Biochimica et Biophysica Acta* **1519**, 153–166.

- Chaves MM, Maroco JP, Pereira J.** 2003. Understanding plant responses to drought – from genes to the whole plant. *Functional Plant Biology* **30**, 239–264.
- Chávez JL, Neale CMU, Prueger JH, Kustas WP.** 2008. Daily evapotranspiration estimates from extrapolating instantaneous airborne remote sensing ET values. *Irrigation Science* **27**, 67–81.
- Chéné Y, Rousseau D, Lucidarme P, Bertheloot J, Caffier V, Morel P, Belin E, Chapeau-Blondeau F.** 2012. On the use of depth camera for 3D phenotyping of entire plants. *Computers Electronics and Agriculture* **82**, 122–127.
- Christensen LK, Rodriguez D, Belford R, Sadras V, Rampant P, Fisher P.** 2005. Temporal prediction of nitrogen status in wheat under the influence of water deficiency using spectral and thermal information. Crop variability and resulting management effects. In: JV Stafford, ed, *Precision agriculture*. The Netherlands: Wageningen Academic Publisher, pp 209–216.
- Cohen Y, Alchanatis V, Meron M, Saranga S, Tsipris J.** 2005. Estimation of leaf water potential by thermal imagery and spatial analysis. *Journal of Experimental Botany* **56**, 1843–1852.
- Costa JM, Ortuño MF, Lopes CM, Chaves MM.** 2012. Grapevine varieties exhibiting differences in stomatal response to water deficit. *Functional Plant Biology* **39**, 179–189.
- Dodd I.** 2013. Absciscic acid and stomatal closure: a hydraulic conductance conundrum? *New Phytologist* **197**, 6–8.
- Ehret DL, Lau A, Bittman S, Lin W, Shelford T.** 2001. Automated monitoring of greenhouse crops. *Agronomie* **21**, 403–414.
- Fedoroff NV, Battisti DS, Beachy RN, et al.** 2010. Radically rethinking agriculture for the 21st century. *Science* **327**, 833–834.
- Flexas J, Galmés J, Gallé A, Gulías J, Pou A, Ribas-Carbo Tomás M, Medrano H.** 2010. Improving water use efficiency in grapevines: potential physiological targets for biotechnological improvement. *Australian Journal of Grape and Wine Research* **16**, 106–121.
- Fuchs M.** 1990. Infrared measurement of canopy temperature and detection of plant water stress. *Theoretical and Applied Climatology* **42**, 253–261.
- Fuentes S, De Bei R, Pech J, Tyerman S.** 2012. Computational water stress indices obtained from thermal image analysis of grapevine canopies. *Irrigation Science* **30**, 523–536.
- Furbank RT, Tester M.** 2011. Phenomics – technologies to relieve the phenotyping bottleneck. *Trends in Plant Science* **16**, 635–644.
- García-Tejero I, Durán-Zuazo VH, Muriel-Fernández JL, Jiménez-Bocanegra JA.** 2011. Linking canopy temperature and trunk diameter fluctuations with other physiological water status tools for water stress management in citrus orchards. *Functional Plant Biology* **38**, 106–117.
- González-Dugo MP, Moran MS, Mateos L, Bryant R.** 2006. Canopy temperature variability as an indicator of crop water stress severity. *Irrigation Science* **24**, 233–240.
- Grant OM, Davies MJ, James CM, Johnson AW, Leinonen I, Simpson DW.** 2012. Thermal imaging and carbon isotope composition indicate variation amongst strawberry (*Fragaria × ananassa*) cultivars in stomatal conductance and water use efficiency. *Environmental and Experimental Botany* **76**, 7–15.
- Grant OM, Tronina L, Jones HG, Chaves MM.** 2007. Exploring thermal imaging variables for the detection of stress responses in grapevine under different irrigation regimes. *Journal of Experimental Botany* **58**, 815–825.
- Gregory PJ, Johnson SN, Newton AC, Ingram JS.** 2009. Integrating pests and pathogens into the climate change/food security debate. *Journal of Experimental Botany* **60**, 2827–2838.
- Grimmer MK, John Foulkes M, Paveley ND.** 2012. Foliar pathogenesis and plant water relations: a review. *Journal of Experimental Botany* **63**, 4321–4331.
- Guilioni L, Jones HG, Leinonen I, Lhomme JP.** 2008. On the relationships between stomatal resistance and leaf temperatures in thermography. *Agricultural and Forest Meteorology* **148**, 1908–1912.
- Hashimoto M, Negi J, Young J, Israelsson M, Schroeder J, Iba K.** 2006. *Arabidopsis* HT1 kinase controls stomatal movements in response to CO<sub>2</sub>. *Nature Cell Biology* **8**, 391–397.
- Havaux M, Triantaphyllides C, Genty B.** 2006. Autoluminescence imaging: a non-invasive tool for mapping oxidative stress. *Trends in Plant Science* **11**, 480–484.
- Henry A, Gowda VR, Torres RO, McNally KL, Serraj R.** 2011. Variation in root system architecture and drought response in rice (*Oryza sativa*): phenotyping of the OryzaSNP panel in rainfed lowland fields. *Field Crops Research* **120**, 205–214.
- Hetherington AM, Woodward I.** 2003. The role of stomata in sensing and driving environmental change. *Nature* **424**, 901–908.
- Jackson RD.** 1986. Remote sensing of biotic and abiotic plant stress. *Annual Review of Phytopathology* **24**, 265–287.
- Jackson RD, Idso SB, Reginato RJ, Pinter PJJ.** 1981. Canopy temperature as a crop water stress indicator. *Water Resources Research* **17**, 1133–1138.
- Jackson RD, Reginato RJ, Idso SB.** 1977. Wheat canopy temperature: a practical tool for evaluating water requirements. *Water Resources Research* **13**, 651–656.
- Jacob F, Schmugge TJ, Olioso A, French A, Courault D, Ogawa K, Petitcolin F, Chehbouni PA, Privette J.** 2008. Modelling and inversion in thermal infrared remote sensing over vegetated land surfaces. In: S Liang, ed, *Advances in land remote sensing: system, modeling, inversion and application*. The Netherlands: Springer, pp 245–292.
- Jiménez-Bello MA, Ballester C, Castel JR, Intrigliolo DS.** 2011. Development and validation of an automatic thermal imaging process for assessing plant water status. *Agricultural Water Management* **98**, 1497–1504.
- Jones HG.** 1992. *Plants and microclimate*, 2nd edn. Cambridge, UK: Cambridge University Press.
- Jones HG.** 1999. Use of thermography for quantitative studies of spatial and temporal variation of stomatal conductance over leaf surfaces. *Plant, Cell and Environment* **22**, 1043–1055.
- Jones HG, Serraj R, Loveys BR, Xiong L, Wheaton A, Price AH.** 2009. Thermal infrared imaging of crop canopies for the remote diagnosis and quantification of plant responses to water stress in the field. *Functional Plant Biology* **36**, 978–979.
- Jones HG, Stoll M, Santos T, de Sousa C, Chaves MM, Grant OM.** 2002. Use of infrared thermography for monitoring stomatal



closure in the field: application to grapevine. *Journal of Experimental Botany* **53**, 1–12.

**Jones HG, Vaughan RA.** 2010. *Remote sensing of vegetation: principles, techniques and applications*. Oxford, UK: Oxford University Press.

**Kaplan H.** 2007. *Practical applications of infrared thermal sensing and imaging equipment*, 3rd ed. Washington, USA: SPIE Press.

**Kerr JT, Ostrovsky M.** 2003. From space to species: ecological applications for remote sensing. *Trends in Ecology and Evolution* **18**, 299–305.

**Kim YH, Lee SH.** 2004. Quality monitoring of potato transplants using thermal and visual images. *Acta Horticulturae* **659**, 273–278.

**Kranner I, Kastberger G, Hartbauer M, Pritchard HW.** 2010. Non-invasive diagnosis of seed viability using infrared thermography. *Proceedings of the National Academy of Sciences, USA* **107**, 3912–3917.

**Kusumi K, Hirotsuka S, Kumamaru T, Iba K.** 2012. Increased leaf photosynthesis caused by elevated stomatal conductance in a rice mutant deficient in SLAC1, a guard cell anion channel protein. *Journal of Experimental Botany* **63**, 5635–5644.

**Lee WS, Alchanatis V, Yang C, Hirafuji M, Moshou D, Li L.** 2010. Sensing technologies for precision specialty crop production. *Computers and Electronics in Agriculture* **74**, 2–33.

**Lefebvre V, Fortabat MN, Ducamp A, North HM, Maia-Grondard A, Trouverie J, Boursiac Y, Mouille G, Durand-Tardif M.** 2011. ESKIMO1 disruption in *Arabidopsis* alters vascular tissue and impairs water transport. *PLoS ONE* **6**, e16645. doi:10.1371/journal.pone.0016645.

**Leinonen I, Grant OM, Tagliavia CPP, Chaves MM, Jones HG.** 2006. Estimating stomatal conductance with thermal imagery. *Plant, Cell and Environment* **29**, 1508–1518.

**Liu Y, Subhasha C, Yana J, Song C, Zhao J, Lia J.** 2011. Maize leaf temperature responses to drought: thermal imaging and quantitative trait loci (QTL) mapping. *Environmental and Experimental Botany* **71**, 158–165.

**Loveys BR, Jones HG, Theobald JC, McCarthy MG.** 2008. An assessment of plant-based measures of grapevine performance as irrigation-scheduling tools. *Acta Horticulturae* **792**, 391–403.

**Lubin DA, Esty DC.** 2010. The sustainability imperative. *Harvard Business Review* May 2010, 1–9.

**Maes WH, Steppe K.** 2012. Estimating evapotranspiration and drought stress with ground-based thermal remote sensing in agriculture: a review. *Journal of Experimental Botany* **63**, 4671–4712.

**Mahlein AK, Oerke EC, Steiner U, Dehne HD.** 2012. Recent advances in sensing plant diseases for precision crop protection. *European Journal of Plant Pathology* **133**, 197–209.

**Melotto M, Underwood W, He SY.** 2008. Role of stomata in plant innate immunity and foliar bacterial diseases. *Annual Review of Phytopathology* **46**, 101–122.

**Merlot S, Leonhardt N, Fenzi F, et al.** 2007. Constitutive activation of a plasma membrane H<sup>+</sup>-ATPase prevents abscisic acid-mediated stomatal closure. *The EMBO Journal* **26**, 3216–3226.

**Merlot S, Mustilli AC, Genty B, North H, Lefebvre V, Sotta B, Vavasseur A, Giraudat J.** 2002. Use of infrared thermal imaging to

isolate *Arabidopsis* mutants defective in stomatal regulation. *The Plant Journal* **30**, 601–609.

**Möller M, Alchanatis V, Cohen Y, Meron M, Tsipris J, Naor A, Ostrovsky V, Sprintsin M, Cohen S.** 2007. Use of thermal and visible imagery for estimating crop water status of irrigated grapevine. *Journal of Experimental Botany* **58**, 827–838.

**Moran MS.** 1994. Irrigation management in Arizona using satellites and airplanes. *Irrigation Science* **15**, 35–44.

**Munns R, James RA, Sirault X, Furbank RT, Jones HG.** 2010. New phenotyping methods for screening wheat and barley for water stress tolerance. *Journal of Experimental Botany* **61**, 3499–3507.

**Negi J, Matsuda O, Nagasawa T, Oba Y, Takahashi H, Kawai-Yamada M, Uchimiya H, Hashimoto M, Iba K.** 2008. CO<sub>2</sub> regulator SLAC1 and its homologues are essential for anion homeostasis in plant cells. *Nature* **452**, 483–486.

**Nilson SE, Assmann SM.** 2007. The control of transpiration. Insights from *Arabidopsis*. *Plant Physiology* **143**, 19–27.

**Nilsson HE.** 1995. Remote sensing and image analysis in plant pathology. *Annual Review of Phytopathology* **15**, 489–527.

**Oerke EC, Steiner U, Dehne HW, Lindenthal M.** 2006. Thermal imaging of cucumber leaves affected by downy mildew and environmental conditions. *Journal of Experimental Botany* **57**, 2121–2132.

**Padhi J, Misra RK, Payero JO.** 2012. Estimation of soil water deficit in an irrigated cotton field with infrared thermography. *Field Crops Research* **126**, 45–55.

**Papdi C, Joseph MP, Salamo IP, Vidal S, Szabados L.** 2009. Genetic technologies for the identification of plant genes controlling environmental stress responses. *Functional Plant Biology* **36**, 696–720.

**Pelleschi S, Leonardi A, Rocher JP, Cornic G, de Vienne D, Thevenot C, Prioul JL.** 2006. Analysis of the relationships between growth, photosynthesis and carbohydrate metabolism using quantitative trait loci (QTLs) in young maize plants subjected to water deprivation. *Molecular Breeding* **17**, 21–39.

**Plessis A, Cournol R, Effroy D, et al.** 2011. New ABA-hypersensitive *Arabidopsis* mutants are affected in loci mediating responses to water deficit and *Dickeya dadantii* infection. *PLoS ONE* **6**, e20243.

**Pramsohler M, Hacker J, Neuner G.** 2012. Freezing pattern and frost killing temperature of apple (*Malus domestica*) wood under controlled conditions and in nature. *Tree Physiology* **32**, 819–828.

**Prohens J, Miro R, Rodriguez-Burruezo A, Chiva S, Verdu G, Nuez F.** 2004. Temperature, electrolyte leakage, ascorbic acid content and sunscald in two cultivars of pepino, *Solanum muricatum*. *Journal of Horticultural Science and Biotechnology* **79**, 375–379.

**Qiu GY, Zhao M.** 2010. Remotely monitoring evaporation rate and soil water status using thermal imaging and ‘three-temperatures model (3T Model)’ under field-scale conditions. *Journal of Environmental Monitoring* **12**, 716–723.

**Roy J, Tucker EJ, Tester M.** 2011. Genetic analysis of abiotic stress tolerance in crops. *Current Opinion in Plant Biology* **14**, 232–239.

**Saji S, Bathula S, Kubo A, et al.** 2008. Disruption of a gene encoding C<sub>4</sub>-dicarboxylate transporter-like protein increases

ozone sensitivity through deregulation of the stomatal response in *Arabidopsis thaliana*. *Plant Cell Physiology* **49**, 2–10.

**Sankaran S, Mishra A, Ehsani R, Davis C.** 2010. A review of advanced techniques for detecting plant diseases. *Computers and Electronics in Agriculture* **72**, 1–13.

**Scherrer D, Badera MK, Körner C.** 2011. Drought-sensitivity ranking of deciduous tree species based on thermal imaging of forest canopies. *Agricultural and Forest Meteorology* **151**, 1632–1640.

**Scherrer D, Körner C.** 2010. Infra-red thermometry of alpine landscapes challenges climatic warming projections. *Global Change Biology* **16**, 2602–2613.

**Scherrer D, Körner C.** 2011. Topographically controlled thermal-habitat differentiation buffers alpine plant diversity against climate warming. *Journal of Biogeography* **38**, 406–416.

**Shimshi D.** 1967. Leaf chlorosis and stomatal aperture. *New Phytologist* **66**, 455–461.

**Sirichandra C, Wasilewska A, Vlad F, Valon C, Leung J.** 2009. The guard cell as a single-cell model towards understanding drought tolerance and abscisic acid action. *Journal of Experimental Botany* **60**, 1439–1463.

**Sobrino JA, Jiménez-Muñoz JC, Zarco-Tejada PJ, et al.** 2009. Thermal remote sensing from airborne hyperspectral scanner data in the framework of the SPARC and SEN2FLEX projects: an overview. *Hydrology and Earth System Sciences* **13**, 2031–2037.

**Stoll M, Schultz HR, Berkelmann-Loehnertz B.** 2008. Thermal sensitivity of grapevine leaves affected by *Plasmopara viticola* and water stress. *Vitis* **47**, 133–134.

**Tardieu F, Simonneau T.** 1998. Variability among species of stomatal control under fluctuating soil water status and evaporative demand: modelling isohydric and anisohydric behaviours. *Journal of Experimental Botany* **49**, 419–432.

**Testi L, Goldhamer DA, Iniesta F, Salinas M.** 2008. Crop water stress index is a sensitive water stress indicator in pistachio trees. *Irrigation Science* **26**, 395–405.

**Thomson SJ, Ouellet-Plamondon CM, DeFauw SL, Huang Y, Fisher DK, English PJ.** 2012. Potential and challenges in use of thermal imaging for humid region irrigation system management. *Journal of Agricultural Science* **4**, 103–116.

**Tilling AK, O'Leary GJ, Ferwerda JG, Jones SD, Fitzgerald GJ, Rodriguez D, Belford R.** 2007. Remote sensing of nitrogen and water stress in wheat. *Field Crops Research* **104**, 77–85.

**Torii T, Kasiwazaki M, Okamoto T, Kitani O.** 1992. Evaluation of graft-take using a thermal camera. *Acta Horticulturae* **319**, 631–634.

**Vollsnies AV, Eriksen AB, Otterholt E, Kvaal K, Oxaal U, Futsaether CM.** 2009. Visible foliar injury and infrared imaging show that daylength affects short-term recovery after ozone stress in *Trifolium subterraneum*. *Journal of Experimental Botany* **60**, 3677–3686.

**Walter A, Studer B, Kölliker R.** 2012. Advanced phenotyping offers opportunities for improved breeding of forage and turf species. *Annals of Botany* **110**, 1271–1279.

**Wilkinson S, Hartung W.** 2009. Food production: reducing water consumption by manipulating long-distance chemical signalling in plants. *Journal of Experimental Botany* **60**, 1885–1891.

**Wisniewski M, Glenn DM, Gusta L, Fuller MP.** 2008. Using infrared thermography to study freezing in plants. *HortScience* **43**, 1648–1651.

**Xie XD, Wang YB, Williamson L, et al.** 2006. The identification of genes involved in the stomatal response to reduced atmospheric relative humidity. *Current Biology* **16**, 882–887.

**Yuan BZ, Sun J, Nishiyama S.** 2004. Effect of drip irrigation on strawberry growth and yield inside a plastic greenhouse. *Biosystems Engineering* **87**, 237–245.

**Zarco-Tejada PJ, González-Dugo V, Berni JAJ.** 2012. Fluorescence, temperature and narrow-band indices acquired from a UAV platform for water stress detection using a micro-hyperspectral imager and a thermal camera. *Remote Sensing of Environment* **117**, 322–337.